NOTES AND CORRESPONDENCE

Approximations and Sensitivity Experiments with a Baroclinic Semi-Lagrangian Spectral Model

HAROLD RITCHIE AND CHRISTIANE BEAUDOIN

Recherche en prévision numérique, Service de l'environnement atmosphérique, Dorval, Quebec, Canada

15 October 1993 and 21 January 1994

ABSTRACT

This study examines the extensions that have been made to a basic semi-Lagrangian semi-implicit multilevel spectral primitive equation model in preparing it for use as an operational data assimilation and medium-range forecast model. The authors present an optimized formulation using accurate approximations to alternate trigonometric calculations for finding the upstream positions and performing the transformations for treating a vector form of the equation of motion in spherical geometry. The impact of the order of accuracy of the interpolators used in the semi-Lagrangian algorithms is also examined. It is shown that the recommended approximations have no significant meteorological consequences, but in a typical model step they reduce the time spent in the semi-Lagrangian calculations from about 50% to about 30%.

Through a series of sensitivity tests, the authors establish the viability of the semi-Lagrangian semi-implicit method for spectral models with a more comprehensive physical parameterization package, and on a wider range of meteorological situations than in the previous study. First of all it is confirmed that even in these global runs with full physical parameterizations the sensitivity to the conversion from an Eulerian to a semi-Lagrangian formulation is acceptably small. In time truncation error tests with a T79 horizontal resolution it is found that, on average and with full physics, 30 min is about the upper limit for the time step based on acceptable time truncation errors. Since the Courant–Friedrichs–Lewy limit for the corresponding Eulerian model is about 10 min and the overhead of the semi-Lagrangian calculations is less than 30% per time step, there is a significant gain in efficiency by using the optimized semi-Lagrangian formulation. Results are also presented showing the improvement in the accuracy of the 5-day forecasts obtained by raising the model top and by increasing the horizontal resolution.

1. Introduction

The efficiency advantage of the semi-Lagrangian semi-implicit time-stepping algorithm was demonstrated a decade ago by Robert (1981, 1982) in the context of gridpoint models of the shallow-water equations. Since that time considerable work has been done in applying the method in baroclinic models, and an increasing number of centers are using it in operational weather forecasting models. One perspective from which to view the development of a numerical technique is to follow its evolution from the stage of its initial demonstration through to its operational implementation. Typically, this involves a sequence of steps: 1) proof of concept in two-dimensional (usually shallow water) models, 2) extension to simple three-dimensional models, 3) coupling with sophisticated physical parameterizations, and 4) final testing and optimization for operational use. Examples of these steps in the context of gridpoint models are for step 1, Robert (1981, 1982), Bates (1984), Staniforth and Temperton (1986), Temperton and Staniforth (1987), Purser and Leslie (1988), McDonald and Bates (1989), and Côté and Staniforth (1990); for step 2, Robert et al. (1985), Tanguay et al. (1990), and Bates et al. (1993); and for steps 3 and 4, Bates and McDonald (1982), McDonald (1986), Tanguay et al. (1989), and McDonald and Haugen (1992, 1993).

The semi-Lagrangian semi-implicit algorithm has now completed a similar evolution for its application on the Gaussian grid used in spectral models. Here step 1 consisted of addressing the geometric and linear stability questions by examining the semi-Lagrangian treatment of advection on the Gaussian calculation grid used in such models (Ritchie 1987), followed by combining the semi-Lagrangian and semi-implicit schemes to get a stable treatment of both Rossby and gravity waves in a spectral model of the shallow-water equations (Ritchie 1988). The extension to a baroclinic model (step 2) was then examined through an application to a multilevel spectral primitive equation

Corresponding author address: Dr. Harold Ritchie, Recherche en prévision numérique, 2121, Trans-Canada Highway, Room 500, Dorval, Quebec, Canada H9P 1J3.

model, where several issues related to vertical discretization were resolved (Ritchie 1991). It was shown that the semi-Lagrangian semi-implicit approach can be applied accurately and stably to produce medium-range (5-day) forecasts in a baroclinic model using time steps that far exceed the Courant–Friedrichs–Lewy (CFL) limit for the corresponding Eulerian model. This was demonstrated by means of intercomparison experiments for a single case using a hemispheric model with simple physical parameterizations. In this study we examine steps 3 and 4. This model has been further developed and implemented as the data assimilation and medium-range forecast model at the Canadian Meteorological Centre. Here we present the main optimization and model configuration extensions that were made in preparing the model for operational use.

Due to the overhead of the extra calculations required by the semi-Lagrangian technique for each time step, the net gain in efficiency can be significantly less than the factor by which the time step is increased. In particular, the previous study (Ritchie 1991) used cubic three-dimensional interpolations throughout and also used very accurate algorithms for the trigonometric calculations in finding the upstream positions, and in the transformations required to treat the vector form of the equation of motion. Section 2 presents some approximations that have significantly increased the efficiency of the semi-Lagrangian calculations without degrading the quality of the forecasts.

It was also important to establish the viability of the semi-Lagrangian semi-implicit time integration scheme with more sophisticated physics parameterizations and on a wider range of meteorological situations than were used in the previous study. In section 3 we examine changes that have been made to the model configuration and assess their impact through a series of sensitivity experiments performed on four First GARP (Global Atmospheric Research Program) Global Experiment (FGGE) cases run with a full-physics parameterization. Here we review the impact of the Eulerian to semi-Lagrangian conversion and then look at time truncation errors, the impact of raising the model's top, and varying the horizontal resolution. A concluding discussion is presented in section 4.

2. Optimized formulation

a. Model formulation

The model formulation is based on the primitive equations expressed in terms of the σ ($= p/p_s$) vertical coordinate (see Ritchie 1991 for details). The total derivatives in these equations are treated using a semi-Lagrangian scheme that avoids vertical interpolation in assessing the field values at the departure points. With this approach a typical primitive equation can be presented as

$$\frac{d_H F}{dt} + \dot\sigma^* \frac{\partial F}{\partial \sigma} + \bar G^t = \left(\overline{R - \dot\sigma \frac{\partial F}{\partial \sigma}}\right)^r + \dot\sigma^* \left(\overline{\frac{\partial F}{\partial \sigma}}\right)^r. \tag{1}$$

Here $\dot\sigma^*$ is the vertical velocity that gives advection to σ^*, the model level nearest the σ value of the departure point at time $t - \Delta t$; $\overline{(\ )}^t$ is a time average that is applied along the trajectory to stabilize the gravity-wave-producing terms (the semi-implicit treatment); and $\overline{(\ )}^r$ is a spatial averaging that is applied to the right-hand-side terms along the trajectory. In addition to reducing a problem related to the pressure gradient terms near mountains, this spatial averaging also provides a significant optimization, as presented in a recent article by Tanguay et al. (1992). If $F(\tau)^+$ indicates the value of F at time τ and grid point $(\mathbf{g}, \sigma_k)$, while $F(t - \Delta t)^-$ indicates its value at time $t - \Delta t$ and upstream position $[\mathbf{r}(t - \Delta t), \sigma^*]$, then using centered approximations for the semi-Lagrangian time derivative, semi-implicit time average, and spatial average leads to

$$\begin{aligned} &F(t + \Delta t)^+ + \Delta t G(t + \Delta t)^+ \\ &= \left[F(t - \Delta t) - \Delta t G(t - \Delta t) \right. \\ &\quad \left. + \Delta t \left(R - \dot\sigma \frac{\partial F}{\partial \sigma} \right)(t) \right]^- + \Delta t \dot\sigma^* \frac{\partial F}{\partial \sigma}(t)^- \\ &\quad + \Delta t \left[\left(R - \dot\sigma \frac{\partial F}{\partial \sigma} \right)(t)^+ + \dot\sigma^* \frac{\partial F}{\partial \sigma}(t)^+ \right]. \end{aligned} \tag{2}$$

The $(\ )^+$ evaluations are at grid points, while the $(\ )^-$ evaluations are at upstream locations that are on model levels but between grid points in the horizontal. Thus, we see that this formulation requires evaluating two two-dimensional interpolations, whereas two three-dimensional (or equivalently eight two-dimensional) interpolations are required for a three-dimensional interpolating version without spatial averaging. Since accurate interpolations are relatively expensive, this spatial averaging is a significant optimization.

Using this as our control model formulation, in the subsequent subsections we will examine the impacts of approximations that significantly increase the efficiency of the semi-Lagrangian calculations without degrading the quality of the forecasts. Although each approximation was tested separately, for brevity we state the impact of using them in various combinations and conclude by showing that combining all the recommended optimizations has negligible meteorological impact.

b. Calculating departure points

As presented in Ritchie (1987), considering position vectors along a great circle trajectory shows that $\mathbf{r}(t - \Delta t)$ can be calculated as

$$\mathbf{r}(t-\Delta t) = 2\left[\mathbf{r}(t)\cdot\frac{\mathbf{g}}{a^2}\right]\mathbf{r}(t) - \mathbf{g}, \qquad (3)$$

where $\mathbf{r}(t)$ is the upstream position at time t and was originally calculated by means of

$$\mathbf{r}(t) = b[\mathbf{g} - \Delta t\dot{\mathbf{r}}(t)] + O(\Delta t^2), \qquad (4)$$

with b being a factor that keeps the trajectory on the sphere. Here $\dot{\mathbf{r}}(t)$ represents the velocity at $\mathbf{r}(t)$, so that (4) is an implicit equation with $\mathbf{r}(t)$ being involved in both the left- and right-hand sides. This equation was solved iteratively, using Cartesian coordinates centered at the center of the sphere, which gave rise to expensive trigonometric functions (two sines, two cosines, one arctangent, and one arcsine) to evaluate on each iteration.

Here we present a modified method that uses spherical trigonometry. If the longitude and latitude corresponding to $\mathbf{g}$, $\mathbf{r}(t)$, and $\mathbf{r}(t-\Delta t)$ are denoted by (λ^+, θ^+), $(\lambda^\circ, \theta^\circ)$, and (λ^-, θ^-), respectively, then (A7)–(A9) of Ritchie (1988) give

$$\sin\theta^\pm = (\sin\theta^\circ)(\cos\alpha) \pm (\cos\theta^\circ)(\sin\alpha)\frac{v}{V} \qquad (5)$$

$$\cos(\lambda^\pm - \lambda^\circ)\cos\theta^\pm = (\cos\theta^\circ)(\cos\alpha) \mp (\sin\theta^\circ)(\sin\alpha)\frac{v}{V} \qquad (6)$$

$$\sin(\lambda^\pm - \lambda^\circ)\cos\theta^\pm = \pm(\sin\alpha)\frac{u}{V}, \qquad (7)$$

where

$$\alpha = \frac{V(t)}{a}\Delta t \qquad (8)$$

and

$$V(t) = [u^2(t) + v^2(t)]^{1/2}, \qquad (9)$$

with $u(t)$ and $v(t)$ being the eastward and northward wind components at $\mathbf{r}(t)$.

Equation (5) can be rewritten as

$$\sin\theta^\pm = A\sin(\theta^\circ \pm \delta), \qquad (10)$$

where

$$A = \left[(\cos^2\alpha) + (\sin^2\alpha)\left(\frac{v}{V}\right)^2\right]^{1/2} \qquad (11)$$

and

$$\delta = \tan^{-1}\left[(\tan\alpha)\frac{v}{V}\right]. \qquad (12)$$

Similarly, (6) can be rewritten as

$$\cos(\lambda^\pm - \lambda^\circ)\cos\theta^\pm = A\cos(\theta^\circ \pm \delta). \qquad (13)$$

Dividing (7) by (13) and using (10) to eliminate $(\theta^\circ \pm \delta)$ gives

$$\lambda^\pm - \lambda^\circ = \pm\tan^{-1}\left\{\frac{(\sin\alpha)u/V}{[\cos^2\theta^\pm - (\sin^2\alpha)u^2/V^2]^{1/2}}\right\}. \qquad (14)$$

As shown in the appendix, Taylor series expansions can be used to develop the following approximations from the relationships. From (A12), (A4), (A14), and (A10), respectively, we have

$$\lambda^\circ = \lambda^+ - \frac{u\Delta t}{a\cos\theta^+}\left[1 + \frac{\Delta t^2}{6a^2}\left(\frac{u^2}{\cos^2\theta^+} - V^2\right)\right] + O(\Delta t^5) \qquad (15)$$

$$\theta^\circ = \theta^+ - \frac{v\Delta t}{a} + \frac{\tan\theta^+}{2}\left(\frac{u\Delta t}{a}\right)^2 + O(\Delta t^3) \qquad (16)$$

$$\lambda^- = \lambda^+ - 2(\sec\theta^+)\frac{u\Delta t}{a}\left[1 - (\tan\theta^+)\left(\frac{v\Delta t}{a}\right)\right] + O(\Delta t^3) \qquad (17)$$

$$\theta^- = \theta^+ - 2\frac{v\Delta t}{a} + \left(\sec^2\theta^+ - \frac{2}{3}\right)\left(\frac{u\Delta t}{a}\right)^2\frac{v\Delta t}{a} + O(\Delta t^4). \qquad (18)$$

Retaining only up to $O(\Delta t)$ terms, these equations correspond to calculating the trajectories directly in (λ, θ) space, which would be a poor approximation near the poles. [See (36), (37) and the associated discussion in Ritchie (1987).] Retaining also the next-order terms gives versions that are much more accurate and that can be calculated much more efficiently than the original algorithms based on Cartesian coordinates.

For typical wind speeds and time steps, the higher-order terms in (15)–(18) are very small except near the poles. We considered the impact of using these approximations for $|\theta^+| < 1.4$ rad (80.2°). In the first test we concentrated on (15) and (16) and retained only the first two terms on the right-hand sides. An integration with this approximation for $|\theta^+| < 80.2°$ was compared to another in which the original formulation based on Cartesian coordinates was used everywhere. The model was run with triangular 79-wave truncation, global domain, 21 levels in the vertical, a 30-min time step, and full-physics parameterization. The integrations started from a FGGE analysis valid at 1200 UTC 12 February 1979, and the evolution of the Northern Hemisphere root-mean-square (rms) differences between the two runs was examined. Although the sensitivity at midaltitudes was less than the usual criterion of 3 m day^{-1}, a marked improvement was achieved by also retaining the remaining terms contained explicitly on the right-hand sides of (15) and (16). It was found that this gives a very accurate ap-

proximation to the original formulation, while eliminating the expensive trigonometric calculations. (Note that $\cos\theta^+$ and $\tan\theta^+$ are Gaussian latitude constants that can be precalculated.)

Approximations (17) and (18) were combined with another modification to the departure point calculations. For a baroclinic model, in the iterative solution of the equations corresponding to (4), the original algorithm used values found on the previous time step as a first guess in the iterative solution:

$$\mathbf{r}_1 = b_0\{\mathbf{g} - \Delta t\mathbf{v}_H[\mathbf{r}(t-\Delta t), \sigma(t-\Delta t), t-\Delta t]\}$$

$$\sigma_1 = \sigma - \Delta t\dot{\sigma}[\mathbf{r}(t-\Delta t), \sigma(t-\Delta t), t-\Delta t].$$

As an alternate approach we can use a "backward first guess" based on winds already available at grid points, giving

$$\mathbf{r}_1 = b_0[\mathbf{g} - \Delta t\mathbf{v}_H(\mathbf{g}, \sigma, t)] \quad (19)$$

$$\sigma_1 = \sigma - \Delta t\dot{\sigma}(\mathbf{g}, \sigma, t). \quad (20)$$

This avoids the storage and input–output costs associated with carrying $[\mathbf{r}(t), \sigma(t)]$ from one time step to the next.

Approximations (15) and (16) can be used in (19), just as they were in (4). We examined the combined effect of using approximations (15) and (16) in (19), and approximations (17) and (18) in place of (3) for $|\theta^+| < 80.2°$. It was found that these approximations are very accurate, while eliminating expensive trigonometric calculations.

c. *Transformation to the tangent Cartesian plane*

To avoid a problem with the metric term in polar regions, the equation of motion is expressed in vector momentum form, as indicated in a study of the shallow-water equations (Ritchie 1988) and examined in detail by Desharnais and Robert (1990). The vector treatment is achieved by transforming to a tangent Cartesian plane and doing the semi-Lagrangian advection in this plane, for which there is no metric term. As presented in (40) and (41) in Ritchie (1988), a key step in this transformation is the calculation of

$$X^\pm = \sin\alpha^\pm \cos\gamma \sin\theta^\circ + (1 - \cos\alpha^\pm)\sin\gamma\cos\gamma\cos\theta^\circ \quad (21)$$

$$Y^\pm = \cos\theta^\circ - \sin\alpha^\pm \sin\gamma \sin\theta^\circ - (1 - \cos\alpha^\pm)\sin^2\gamma\cos\theta^\circ, \quad (22)$$

where α is given by (8) and

$$\gamma = \tan^{-1}\left[\frac{v(t)}{u(t)}\right]. \quad (23)$$

The original scheme used spherical trigonometry to calculate the great circle angle α based on (λ^+, θ^+), $(\lambda^\circ, \theta^\circ)$, but a good approximation for typical wind speeds and time steps used in NWP models is obtained by approximating $\cos\alpha$ by 1 and $\sin\alpha$ by α, leading to

$$X^\pm = \pm\Delta t\frac{u(t)}{a}\sin\theta^\circ + O(\Delta t^2) \quad (24)$$

$$Y^\pm = \cos\theta^\circ \mp \Delta t\frac{v(t)}{a}\sin\theta^\circ + O(\Delta t^2). \quad (25)$$

d. *Orders of interpolators*

With the formulation given by (2), the only remaining three-dimensional interpolations are those used in the calculation of the upstream locations $[\mathbf{r}(t), \sigma^*(t)]$ as described in Ritchie (1991), where tricubic interpolation was used. We tested the impact of reducing the accuracy of the vertical interpolation from cubic to linear, while retaining bicubic in the horizontal, and found that the meteorological impact was negligible.

For the horizontal interpolations we reduced the accuracy from cubic to linear on the first iteration and quadratic on the second, as justified by McDonald (1987). This also had negligible meteorological impact, and all the optimizations discussed up to this point were accepted for operational implementation. Another optimization tested was to use linear interpolation in the horizontal on both iterations. Although the impact of this change was well below the criterion of 3 m day^{-1}, it was considerably larger than for the other optimizations, and hence was not implemented.

To conclude this section, in Fig. 1 we show the impact of combining all the approximations presented here [approximations (15)–(18) used for $|\theta| < 80.2°$, (24) and (25) using the backward first guess (19) and

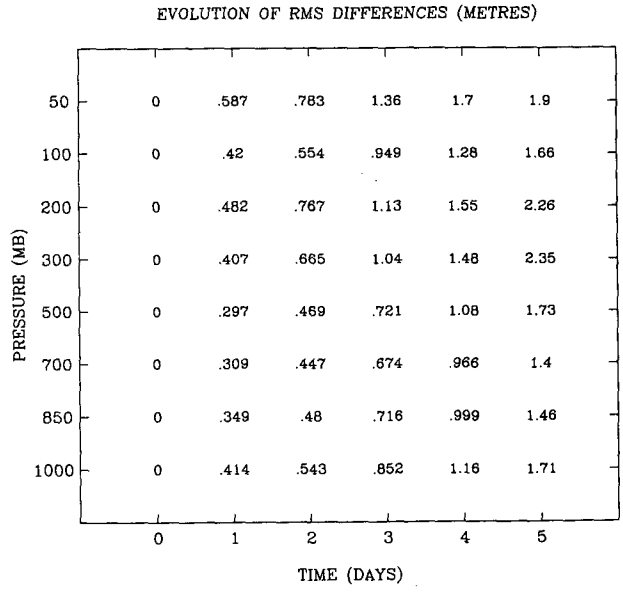

FIG. 1. Evolution of the Northern Hemisphere rms differences (m) due to using all the recommended approximations.

(20), and, in the trajectory calculation, using linear interpolation in the vertical and linear interpolation in the horizontal on the first iteration followed by quadratic interpolation on the second iteration]. It is seen that the sensitivity is less than 0.5 m day^{-1}, which is very small. The 120-h mean sea level pressure forecasts for the Northern Hemisphere produced by the control model and the model with all the recommended approximations are shown in Figs. 2 and 3, respectively. The differences are barely perceptible.

These approximations have no significant meteorological consequences but in a typical semi-Lagrangian model step they reduce the time spent in the semi-Lagrangian calculations from about 50% to about 30%. It should also be kept in mind that replacing an Eulerian treatment of advection by a semi-Lagrangian one removes some expensive spectral transforms required for the Eulerian formulation. Thus, the overhead of the optimized semi-Lagrangian computations is far more than offset by the increase (a factor of between 2.5 and 3 for this T79 model) that they permit in the size of the time step.

Optimizing and multitasking this semi-Lagrangian spectral model enabled it to respect the operational deadlines at the Canadian Meteorological Centre and to be implemented as the global data assimilation and medium-range forecast model on 12 March 1991. Even greater efficiencies are anticipated with further increases in spatial resolution that would impose more stringent CFL time-step restrictions in Eulerian models.

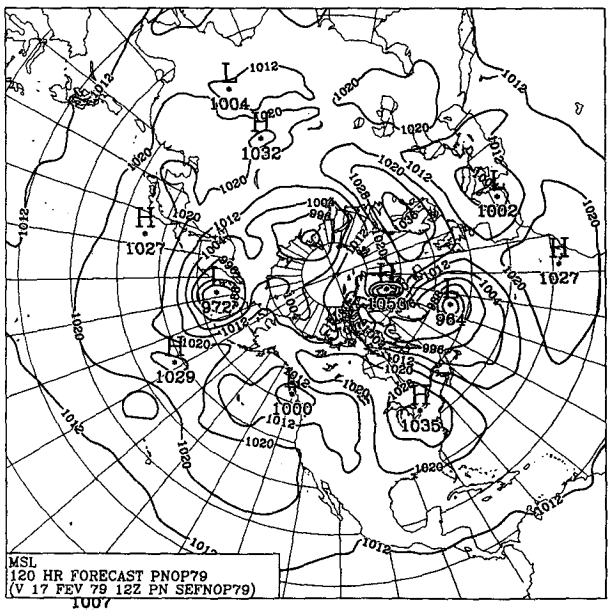

FIG. 2. The 120-h forecast of mean sea level pressure for the Northern Hemisphere produced by the control model. The contour interval is 8 mb.

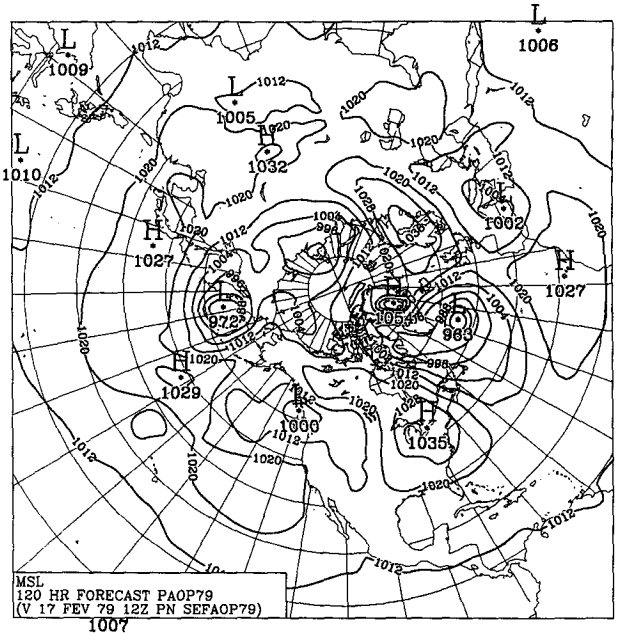

FIG. 3. As in Fig. 2 except produced by the model with all the recommended approximations.

3. Model configuration sensitivity tests

The previous experiments with a semi-Lagrangian semi-implicit multilevel spectral primitive equation model dealt with a single case using a hemispheric model with simple parameterizations (Ritchie 1991). In this section we examine the main extensions made to this model in preparing it for implementation as the data assimilation and medium-range forecast model at the Canadian Meteorological Centre. This is done for a global model with a more sophisticated physics parameterizations and on a wider range of meteorological situation than were used in the previous study. In the following we present results for the Northern Hemisphere averaged over four FGGE cases: 2 January, 21 January, 12 February, and 18 May 1979. The control model has triangular 79-wave truncation in the horizontal and 21 levels with variable spacing in the vertical, and uses the semi-implicit semi-Lagrangian time integration scheme with a 30-min time step. A Robert time filter [with a coefficient of 0.1 using the definition given in the analysis by Asselin (1972)] and a horizontal diffusion ($10^5\nabla^2$ form) are also applied. This dynamical model is coupled with a physical parameterization that includes a planetary boundary layer based on turbulent kinetic energy, a surface layer based on similarity theory, solar and infrared radiation, large-scale precipitation, Manabe-type moist convection, and gravity wave drag (see Girard et al. 1991 for more detail). The sigma levels are placed at 0.010, 0.045, 0.090, 0.140, 0.190, 0.245, 0.304, 0.366, 0.430, 0.494, 0.558, 0.622, 0.684, 0.744, 0.800, 0.850, 0.894, 0.932,

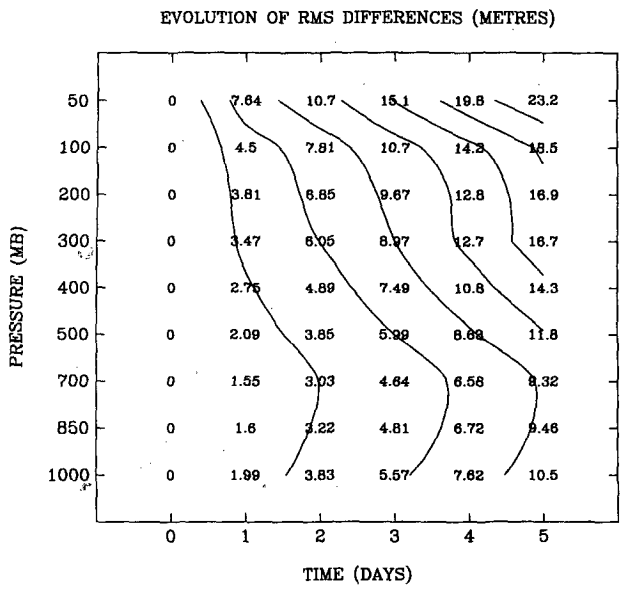

FIG. 4. Average (over four cases) of the evolution of the Northern Hemisphere rms differences (m) between forecasts produced by the semi-Lagrangian model and an Eulerian version, both using a 10-min time step.

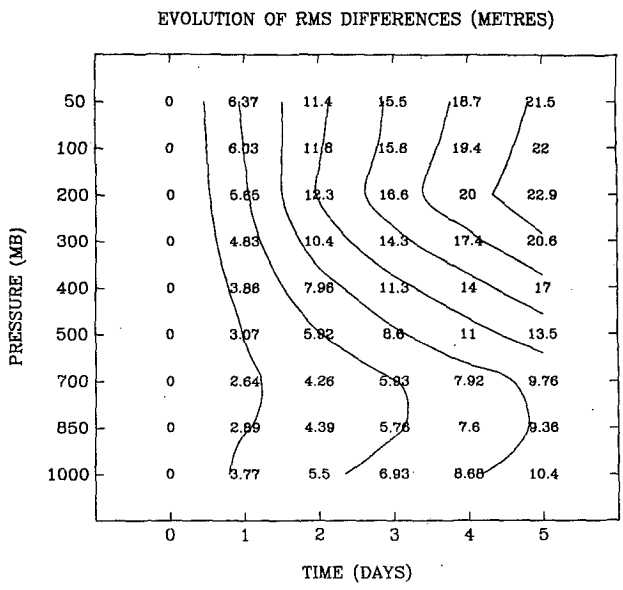

FIG. 5. As in Fig. 4 except for differences between semi-Lagrangian runs using a 10-min time step and a 30-min time step.

0.964, 0.990, and 1.00. Notice the closer spacing near the surface in order to better resolve the boundary layer processes.

a. Eulerian to semi-Lagrangian conversion

Figure 4 shows the evolution of the Northern Hemisphere rms difference between the semi-Lagrangian version of the model as presented in section 2a and an Eulerian version of the model, both using a 10-min time step. It is seen that, even in these global runs with full physical parameterizations, the Eulerian to semi-Lagrangian conversion satisfies the sensitivity criterion of less than 3 m day^{-1} at midatmospheric levels.

b. Time step

Figure 5 shows the evolution of the Northern Hemispheric rms difference between semi-Lagrangian runs using a 10-min and a 30-min time step, averaged over the four cases. This result suggests that, on average and with full physics, 30 min is currently about the upper limit for the time step based on acceptable time truncation errors, whereas a time step of 40 min was acceptable with simpler parameterizations (Ritchie 1991). The CFL limit for the corresponding Eulerian model is about 10 min, and the overhead of the semi-Lagrangian calculations is about 30%, as discussed in section 2, so that there is a significant gain in efficiency.

c. Raising the top

The control model has its top two levels at $\sigma_1 = 0.010$ and $\sigma_2 = 0.045$, whereas the model used in Ritchie (1991) has its top at $\sigma = 0.050$. Here we test the impact of the position of the top by removing the level at $\sigma = 0.010$. Figure 6 presents the vertical profiles of the rms deviations (compared to analyses, biases removed) of the 5-day geopotential height forecasts. The solid curve is for the runs with the top at $\sigma_1 = 0.010$, and the dashed curve is for the runs with the

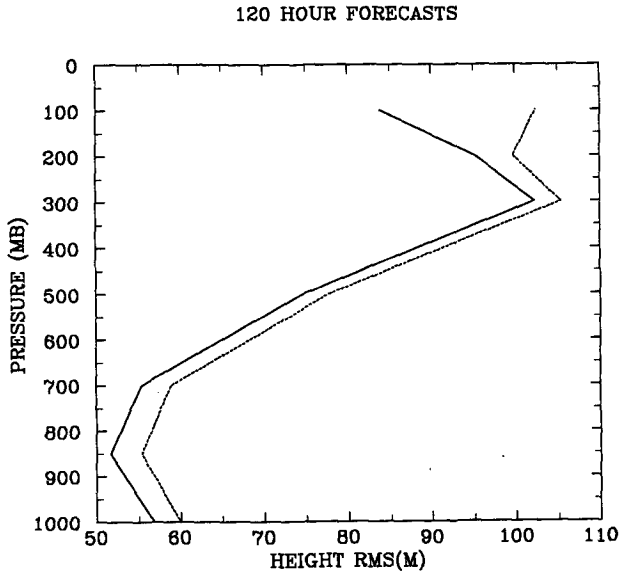

FIG. 6. Average (over four cases) of the vertical profiles of the rms deviations (m, compared to analyses, biases removed) of the 5-day geopotential height forecasts. The solid curve is for the runs with the top at $\sigma = 0.010$, and the dashed curve is for runs with the top at 0.045.

top at $\sigma_1 = 0.045$. The profiles for the corresponding biases showed very little impact resulting from this change (figure not shown). From Fig. 6 it is seen that the presence of the level at $\sigma = 0.010$ produces a significant improvement in the accuracy of the forecasts, especially in the stratosphere.

This is consistent with the results of Mechoso et al. (1982) based on intercomparing models with tops at 1 and 51.8 mb. They found significant errors appearing in the ultralong waves within the first 5 days in the model with the top at 51.8 mb. Boville and Baumhefner (1990) got a more specific measure of the impact of a model top at about $\sigma = 0.010$. They assessed the effect of the upper stratosphere (between 0.025 mb and 10 mb) and concluded that its removal does not seem to lead to significant error development in the troposphere for at least 10 days. However, systematic errors in the troposphere develop primarily after 20 days. Thus, it is likely that our current choice of $\sigma_1 = 0.010$ will be adequate for medium-range forecasts but that it will be necessary to raise the top further for extended-range prediction.

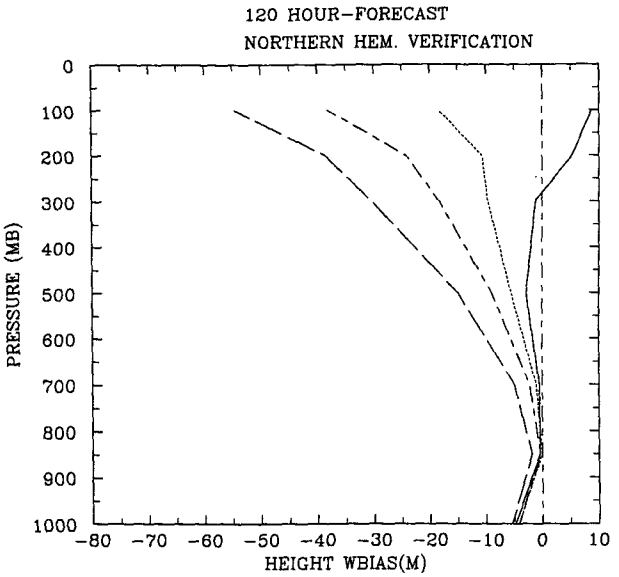

FIG. 7. As in Fig. 6 except for geopotential height biases at various horizontal resolutions: T59 (long dashed), T79 (variably dashed), T99 (short dashed), and T119 (solid).

d. Horizontal resolution

The control model has triangular 79-wave truncation (T79) in the horizontal, whereas the former operational model at the Canadian Meteorological Centre was run at T59. The sensitivity to horizontal resolution was tested by comparing the control model integrations to others run at T59, T99, and T119. In performing these experiments, the ∇^2 horizontal diffusion was adjusted to give the same e-folding time for the shortest resolvable scale. This yielded coefficients ($\times 10^5$ m^2 s^{-1}) of 1.78 at T59, 1.00 at T79, 0.64 at T99, and 0.44 at T119. The main impact was found to be in the geopotential height biases, for which the day 5 profiles are presented in Fig. 7, where the variably dashed curve is for the T79 control model, the long dashed curve is for T59 resolution, the short dashed curve is for T99 resolution, and the solid curve is for T119 resolution. It is seen that there was improvement in going from T59 to T79 and that there is still more improvement to come with further increasing the resolution to T119 and perhaps beyond.

4. Discussion

This study has examined the extensions that have been made to a basic semi-Lagrangian semi-implicit multilevel spectral primitive equation model (Ritchie 1991) in preparing it for use as an operational data assimilation and medium-range forecast model. In section 2 we presented an optimized formulation using accurate approximations to alternate trigonometric calculations for finding the upstream positions and performing the transformations for treating a vector form of the equation of motion in spherical geometry. The impact of the order of accuracy of the interpolators used in the semi-Lagrangian algorithms was also examined. It was shown that the recommended approximations have no significant meteorological consequences, but in a typical model step they reduce the time spent in the semi-Lagrangian calculations from about 50% to about 30%.

Through a series of sensitivity tests, in section 3 we established the viability of the semi-Lagrangian semi-implicit method for spectral models with a more comprehensive physical parameterization package, and on a wider range of meteorological situations than in the previous study. First of all it was confirmed that, even in these global runs with full physical parameterizations, the sensitivity to the conversion from an Eulerian to a semi-Lagrangian formulation is acceptably small. In time truncation error tests with a T79 horizontal resolution it was found that, on average and with full physics, 30 min is about the upper limit for the time step based on acceptable time truncation errors. Since the CFL limit for the corresponding Eulerian model is about 10 min and the overhead of the semi-Lagrangian calculations is less than 30% per time step, there is a significant gain in efficiency by using the optimized semi-Lagrangian formulation. Results were also presented showing the improvement in the accuracy of the 5-day forecasts obtained by raising the model top and by increasing the horizontal resolution from T59 to T79, T99, and T119. The T79 version of this semi-Lagrangian spectral model was implemented as the global data assimilation and medium-range forecast model at the Canadian Meteorological Centre on 12

March 1991, and the resolution was increased to T119 on 17 June 1993.

Due to the more stringent CFL time-step restriction in the corresponding Eulerian models, semi-Lagrangian versions of spectral models produce even greater efficiencies with further increases in resolution. These semi-Lagrangian algorithms have been incorporated in the European Centre for Medium-Range Weather Forecasts forecast model and implemented operationally in a T213L31 version on 17 September 1991. The necessary adaptation and resulting high-resolution performance is the subject of an upcoming paper.

Acknowledgments. The authors are grateful to colleagues at RPN, CMC, and ECMWF for helpful discussions during the course of this work. The approximations for the trajectory calculations presented in section 2b were derived by the first author during a short visit to ECMWF in the autumn of 1990. Thanks are also expressed to Diane Lespérance for typing the manuscript and to Monique Tanguay for reviewing it.

APPENDIX

Taylor Series Approximations for Trajectory Calculation

For the latitudinal positions, (10) gives

$$\theta^\circ = \sin^{-1}\left(\frac{\sin\theta^\pm}{A}\right) \mp \delta. \tag{A1}$$

Equations (8), (9), (11), and the Taylor series expansions for $\sin\alpha$ and $\cos\alpha$ lead to

$$A = \left[1 - \left(\frac{u\Delta t}{a}\right)^2\right]^{1/2} + O(\Delta t^4). \tag{A2}$$

Equations (8), (9); (12), and the Taylor series expansions for $\tan\alpha$ and $\tan^{-1}$ show

$$\delta = \frac{v\Delta t}{a} + \frac{1}{3}\left(\frac{u\Delta t}{a}\right)^2 \frac{v\Delta t}{a} + O(\Delta t^5). \tag{A3}$$

Developing the Taylor series expansion for

$$\sin^{-1}\left[\frac{\sin\theta^\pm}{(1-\epsilon_1)^{1/2}}\right] \quad \text{where} \quad \epsilon_1 = \left(\frac{u\Delta t}{a}\right)^2$$

from (A2) and substituting along with (A3) into (A1) gives

$$\theta^\circ = \theta^\pm \mp \frac{v\Delta t}{a} + \frac{\tan\theta^\pm}{2}\left(\frac{u\Delta t}{a}\right)^2 \mp \frac{1}{3}\left(\frac{u\Delta t}{a}\right)^2 \frac{v\Delta t}{a} + O(\Delta t^4). \tag{A4}$$

This can be used to find θ° from θ^+.

From (A4) we find

$$(\theta^+ - \theta^-) + \frac{\tan\theta^+ - \tan\theta^-}{2}\left(\frac{u\Delta t}{a}\right)^2 + O(\Delta t^4) = 2\frac{v\Delta t}{a} + \frac{2}{3}\left(\frac{u\Delta t}{a}\right)^2 \frac{v\Delta t}{a}. \tag{A5}$$

From the addition formula for tan,

$$\tan\theta^+ - \tan\theta^- = (1 + \tan\theta^+ \tan\theta^-)\tan(\theta^+ - \theta^-). \tag{A6}$$

From (A5) it follows that

$$\tan(\theta^+ - \theta^-) = 2\frac{v\Delta t}{a} + O(\Delta t^2). \tag{A7}$$

Also from (A5) we deduce

$$\tan\theta^- = \tan(\theta^+ - \epsilon_2), \tag{A8}$$

where $\epsilon_2 = 2(v\Delta t/a) + \cdots$.

Doing a Taylor series expansion for (A8) yields

$$\tan\theta^- = \tan\theta^+ - 2(\sec^2\theta^+)\left(\frac{v\Delta t}{a}\right) + O(\Delta t^2). \tag{A9}$$

Substituting (A9) in (A5) and solving for θ^- yields

$$\theta^- = \theta^+ - 2\frac{v\Delta t}{a} + \left(\sec^2\theta^+ - \frac{2}{3}\right)\left(\frac{u\Delta t}{a}\right)^2 \frac{v\Delta t}{a} + O(\Delta t^4). \tag{A10}$$

This can be used to find θ^- from θ^+.

For the longitudinal position, the right-hand side of (14) involves

$$\tan^{-1}\left[\frac{\epsilon_3}{(1-\epsilon_3^2)^{1/2}}\right], \tag{A11}$$

where $\epsilon_3 = (\cos\theta^\pm)^{-1}(\sin\alpha)\, u/V$.

After using (8), (9), and the Taylor series expansions in (A11), (14) becomes

$$\lambda^\pm - \lambda^\circ = \pm\frac{u\Delta t}{a\cos\theta^\pm}\left[1 + \frac{\Delta t^2}{6a^2}\left(\frac{u^2}{\cos^2\theta^\pm} - V^2\right)\right] + O(\Delta t^5). \tag{A12}$$

This can be used to find λ° from (λ^+, θ^+).

It also implies

$$\lambda^+ - \lambda^- = \frac{u\Delta t}{a}(\sec\theta^+ + \sec\theta^-) + \frac{1}{6}\left(\frac{u\Delta t}{a}\right)^3 \times (\sec^3\theta^+ + \sec^3\theta^-) - \frac{1}{6}\frac{u\Delta t}{a}\left(\frac{V\Delta t}{a}\right)^2 \times (\sec\theta^+ + \sec\theta^-) + O(\Delta t^5). \tag{A13}$$

From (A10) $\theta^- = \theta^+ + \epsilon_4$ where

$$\epsilon_4 = -2\frac{v\Delta t}{a} + \left(\sec^2\theta^+ - \frac{2}{3}\right)\left(\frac{u\Delta t}{a}\right)^2\frac{v\Delta t}{a} + O(\Delta t^4),$$

so $\sec\theta^- = \sec(\theta^+ + \epsilon_4)$, which, after developed as a Taylor series in ϵ_4, gives

$$\sec\theta^- = \sec\theta^+ - 2(\sec\theta^+)(\tan\theta^+)\left(\frac{v\Delta t}{a}\right) + 2(\sec\theta^+)(\sec^2\theta^+ + \tan^2\theta^+)\left(\frac{v\Delta t}{a}\right)^2 + O(\Delta t^3).$$

Using this in (A13) produces

$$\lambda^- = \lambda^+ - \frac{u\Delta t}{a}\left\{2\sec\theta^+ - \frac{v\Delta t}{a}\left[2\sec\theta^+\tan\theta^+ - 2\sec\theta^+(\sec^2\theta^+ + \tan^2\theta^+)\left(\frac{v\Delta t}{a}\right)\right] + \frac{1}{3}\sec^3\theta^+\left(\frac{u\Delta t}{a}\right)^2 - \frac{1}{3}\sec\theta^+\left(\frac{V\Delta t}{a}\right)^2\right\} + O(\Delta t^4). \quad \text{(A14)}$$

This can be used to find λ^- from (λ^+, θ^+).

REFERENCES

Asselin, R., 1972: Frequency filter for time integrations. *Mon. Wea. Rev.*, **100,** 487–490.

Bates, J. R., 1984: An efficient semi-Lagrangian and alternating-direction implicit method for integrating the shallow-water equations. *Mon. Wea. Rev.*, **112,** 2033–2047.

——, and A. McDonald, 1982: Multiply-upstream, semi-Lagrangian advective schemes: Analysis and application to a multilevel primitive equation model. *Mon. Wea. Rev.*, **110,** 1831–1842.

——, S. Moorthi, and R. W. Higgins, 1993: A global multilevel atmospheric model using a vector semi-Lagrangian finite-difference scheme. Part I: Adiabatic formulation. *Mon. Wea. Rev.*, **121,** 244–263.

Boville, B. A., and D. P. Baumhefner, 1990: Simulated forecast error and climate drift resulting from the omission of the upper stratosphere in numerical models. *Mon. Wea. Rev.*, **118,** 1517–1530.

Côté, J., and A. Staniforth, 1990: An accurate and efficient finite-element global model of the shallow-water primitive equations. *Mon. Wea. Rev.*, **118,** 2707–2717.

Desharnais, F., and A. Robert, 1990: Errors near the poles generated by a semi-Lagrangian integration scheme in a global spectral model. *Atmos. Ocean,* **28,** 162–176.

Girard, C., Y. Delage, J. Mailhot, L. Garand, B. Bilodeau, N. Brunet, and G. Pellerin, 1991: Physical parameterization for the first Canadian global forecast model. *Extended Abstracts, Ninth Conf. on Numerical Weather Prediction,* Denver, Amer. Meteor. Soc., 502–505.

McDonald, A., 1986: A semi-Lagrangian and semi-implicit two time level integration scheme. *Mon. Wea. Rev.*, **114,** 824–830.

——, 1987: Accuracy of multiply-upstream semi-Lagrangian advective schemes II. *Mon. Wea. Rev.*, **115,** 1446–1450.

——, and J. R. Bates, 1989: Semi-Lagrangian integration of a gridpoint shallow-water model on the sphere. *Mon. Wea. Rev.*, **117,** 130–137.

——, and J. E. Haugen, 1992: A two time-level, three-dimensional semi-Lagrangian, semi-implicit, limited-area gridpoint model of the primitive equations. *Mon. Wea. Rev.*, **120,** 2603–2621.

——, and ——, 1993: A two time-level, three-dimensional semi-Lagrangian, semi-implicit, limited-area gridpoint model of the primitive equations. Part II: Extension to hybrid vertical coordinates. *Mon. Wea. Rev.*, **121,** 2077–2087.

Mechoso, C. R., M. J. Saurez, K. Yamazaki, J. A. Spahr, and A. Arakawa, 1982: A study of the sensitivity of numerical forecasts to an upper boundary in the lower stratosphere. *Mon. Wea. Rev.*, **110,** 1984–1993.

Purser, R. J., and L. M. Leslie, 1988: A semi-implicit semi-Lagrangian finite-difference scheme using high-order spatial differencing on a nonstaggered grid. *Mon. Wea. Rev.*, **116,** 2069–2080.

Ritchie, H., 1987: Semi-Lagrangian advection on a Gaussian grid. *Mon. Wea. Rev.*, **115,** 608–619.

——, 1988: Application of the semi-Lagrangian method to a spectral model of the shallow water equations. *Mon. Wea. Rev.*, **116,** 1587–1598.

——, 1991: Application of the semi-Lagrangian method to a multilevel spectral primitive-equations model. *Quart. J. Roy. Meteor. Soc.*, **117,** 91–106.

Robert, A., 1981: A stable numerical integration scheme for the primitive meteorological equations. *Atmos. Ocean,* **19,** 35–46.

——, 1982: A semi-Lagrangian and semi-implicit numerical integration scheme for the primitive meteorological equations. *J. Meteor. Soc. Japan,* **60,** 319–325.

——, T. L. Yee, and H. Ritchie, 1985: A semi-Lagrangian and semi-implicit numerical integration scheme for multilevel atmospheric models. *Mon. Wea. Rev.*, **113,** 388–394.

Staniforth, A., and C. Temperton, 1986: Semi-implicit semi-Lagrangian integration schemes for a barotropic finite-element regional model. *Mon. Wea. Rev.*, **114,** 2078–2090.

Tanguay, M., A. Simard, and A. Staniforth, 1989: A three-dimensional semi-Lagrangian scheme for the Canadian regional finite-element forecast model. *Mon. Wea. Rev.*, **117,** 1861–1871.

——, A. Robert, and R. Laprise, 1990: A semi-implicit semi-Lagrangian fully compressible regional forecast model. *Mon. Wea. Rev.*, **118,** 1970–1980.

——, E. Yakimiw, H. Ritchie, and A. Robert, 1992: Advantages of spatial averaging in semi-Lagrangian schemes. *Mon. Wea. Rev.*, **120,** 113–123.

Temperton, C., and A. Staniforth, 1987: An efficient two-time-level semi-Lagrangian semi-implicit integration scheme. *Quart. J. Roy. Meteor. Soc.*, **113,** 1025–1039.